Chondroitin 4-*O*-sulfotransferase-1 is required for somitic muscle development and motor axon guidance in zebrafish

Shuji MIZUMOTO*†[1], Tadahisa MIKAMI*[1,2], Daiki YASUNAGA*, Naoki KOBAYASHI*, Hajime YAMAUCHI‡, Ayumi MIYAKE‡, Nobuyuki ITOH‡, Hiroshi KITAGAWA* and Kazuyuki SUGAHARA*†[2]

*Department of Biochemistry, Kobe Pharmaceutical University, Higashinada-ku, Kobe 658-8558, Japan, †Laboratory of Proteoglycan Signaling and Therapeutics, Graduate School of Life Science, Hokkaido University, Frontier Research Center for Post-Genomic Science and Technology, Nishi 11-choume, Kita 21-jo, Kita-ku, Sapporo, Hokkaido 001-0021, Japan, and ‡Department of Genetic Biochemistry, Kyoto University of Graduate School of Pharmaceutical Sciences, Yoshida-Shimoadachi, Sakyo-ku, Kyoto 606-8501, Japan

CS (chondroitin sulfate) has been implicated in a variety of biological processes during development. Its biological functions are closely associated with characteristic sulfated structures. Here, we report the characterization of a zebrafish counterpart of *C4ST-1* (chondroitin 4-*O*-sulfotransferase-1) and its functional importance in embryogenesis. Recombinant C4ST-1 showed a substrate preference for chondroitin and catalysed the 4-O-sulfation of GalNAc residues, a highly frequent modification of CS in the embryos of zebrafish as well as other vertebrates. Whole-mount *in situ* hybridization revealed that *C4ST-1* showed a distinct spatiotemporal expression pattern in the developing zebrafish embryo. During the segmentation stages, strong expression was observed along the body axis including the notochord and somites. Functional knockdown of *C4ST-1* with specific antisense morpholino-oligonucleotides led to a marked decrease in the 4-O-sulfation and amount of CS in the embryos. Consistent with the preferential expression in the rostrocaudal axis, *C4ST-1* morphants displayed morphological defects exemplified by a ventrally bent trunk and a curled and/or kinky tail, largely due to misregulated myotomal *myod* expression, implying perturbation of axial muscle differentiation in somites. Furthermore, the aberrant projection of spinal motor axons, which extended ventrally at the interface between the notochord and individual somites, was also observed in *C4ST-1* morphants. These results suggest that 4-O-sulfated CS formed by C4ST-1 is essential for somitic muscle differentiation and motor axon guidance in zebrafish development.

Key words: chondroitin sulfate, embryogenesis, glycosaminoglycan, sulfation, sulfotransferase, zebrafish.

INTRODUCTION

CS (chondroitin sulfate), one of the major sulfated GAGs (glycosaminoglycans), is ubiquitously distributed at the cell surface and in extracellular matrices as PGs (proteoglycans), in which CS chains are covalently attached to a panel of core proteins [1]. Mounting evidence suggests a substantial contribution of CS moieties to various physiological functions of CS-PGs such as cytokinesis, neuronal network formation, morphogenesis and infections with viruses and bacteria [2–5]. The chondroitin backbone is composed of repetitive disaccharide units [GlcA-GalNAc]$_n$. The building blocks can be replaced with sulfate groups at various positions, mainly at the C-2 position of GlcA and at the C-4 and/or C-6 positions of GalNAc residues, in various combinations, thereby producing characteristic sulfation patterns and structural heterogeneity [3,5]. The sulfation profiles are spatiotemporally tuned during development [6–8]. *In vitro* studies over the past decade have demonstrated that CS polymers and oligosaccharides possess neuroregulatory functions such as neuronal cell adhesion and neurite outgrowth, and interact with a wide range of signalling molecules including Hep (heparin)-binding growth factors in a sulfation-dependent manner [2,3,9,10], suggesting that CS chains differing in sulfation position and degree perform distinct functions *in vivo*.

In biosynthesis, the structural variability of CS is generated under the control of multiple sulfotransferases, and GlcA C-5-epimerase(s) that catalyse the epimerization of GlcA to IdoA (iduronic acid), converting CS into its stereoisomer DS (dermatan sulfate) [5,11,12]. Since each biosynthetic enzyme also exhibits a cell-type-specific and tissue-specific pattern of expression, substantial heterogeneity exists even in CS isolated from a single species. 4-O-sulfation of GalNAc residues is a typical modification found in CS/DS at higher frequency in vertebrates. To date, four phylogenetically related sulfotransferases, C4ST-1 (chondroitin 4-*O*-sulfotransferase-1), C4ST-2, C4ST-3 and D4ST-1 (dermatan 4-*O*-sulfotransferase-1), responsible for the 4-O-sulfation of CS/DS have been identified and characterized in mammals [13–17]. All these enzymes except C4ST-3 show broad, overlapping mRNA tissue distributions [13–16], and therefore are assumed to be, at least in part, functionally redundant, providing a plausible explanation for a predominance of the 4-O-sulfation over the other sulfations, each of which is catalysed by a single or two specific sulfotransferases [5,11]. However, a single deficiency in *C4ST-1* in sog9 cells, a mouse L cell mutant, has been demonstrated to

Abbreviations used: 2-AB, 2-aminobenzamide; BMP, bone morphogenetic protein; C4ST, chondroitin 4-*O*-sulfotransferase; CS, chondroitin sulfate; DAB, diaminobenzidine; D4ST, dermatan 4-*O*-sulfotransferase; DS, dermatan sulfate; EST, expressed sequence tag; GAG, glycosaminoglycan; Hep, heparin; hpf, hours post fertilization; HS, heparan sulfate; IdoA, iduronic acid; MO, morpholino-oligonucleotide; PAPS, 3′-phosphoadenosine 5′-phosphosulfate; PFA, paraformaldehyde; PG, proteoglycan; sema5A, semaphorin 5A; ΔHexA, 4,5-unsaturated hexuronic acid or 4-deoxy-α-L-*threo*-hex-4-enepyranosyluronic acid; ΔDi-0S, $\Delta^{4,5}$HexAα1–3GalNAc; ΔDi-4S, $\Delta^{4,5}$HexAα1–3GalNAc(4-*O*-sulfate); ΔDi-6S, $\Delta^{4,5}$HexAα1–3GalNAc(6-*O*-sulfate); ΔDi-diS_D, $\Delta^{4,5}$HexA(2-*O*-sulfate)α1–3GalNAc(6-*O*-sulfate); ΔDi-diS_E, $\Delta^{4,5}$HexAα1–3GalNAc(4,6-*O*-disulfate); ΔDi-triS, $\Delta^{4,5}$HexA(2-*O*-sulfate)α1–3GalNAc(4,6-*O*-disulfate).

[1] These authors have contributed equally to this work.

[2] Correspondence may be addressed to either of these authors (email tmikami@kobepharma-u.ac.jp or k-sugar@sci.hokudai.ac.jp).

The nucleotide sequence reported in this paper will appear in GenBank®, EMBL, DDBJ and GSDB Nucleotide Sequence Databases under the accession numbers AB097217, AB122017 and AB089140 for zebrafish C4ST-1, C4ST-2 and D4ST-1 respectively.

lead to a drastic decrease in the 4-O-sulfated structures and the amount of CS [18]. In addition, Klüppel et al. [19] have previously reported that a gene trap mutation of *C4ST-1* in mice causes severe chondrodysplasia characterized by a disorganized growth plate as well as specific alterations in the orientation of chondrocyte columns, where a strong reduction in 4-O-sulfated CS occurs. These findings suggest that C4ST-1 contributes substantially to the *in vivo* construction of 4-O-sulfated CS, and that the resultant CS plays crucial roles in embryonic development and physiological phenomena. However, despite the widespread expression of *C4ST-1*, additional phenotypic features resulting from loss of function of *C4ST-1* were not found, largely due to neonatal lethality with respiratory distress in the *C4ST-1*-deficient mice [19].

The zebrafish is an emerging model system for the study of vertebrate development and diseases [20], because of its well-characterized embryonic morphogenesis and suitability for forward and reverse genetics [21]. In zebrafish embryos, intense CS immunoreactivity was originally detected in the spinal cord and at the interface between the notochord and individual somites, where spinal motor axons extend ventrally to establish the midsegmental ventral motor nerves innervating the somatic musculature [22]. The labelled regions include at least two important embryonic structures, somites and peripheral spinal motor axons, both of which are formed as repetitive, morphologically similar units along the body axis through the segmentation processes that commonly occur during vertebrate development. Enzymatic removal of CS by injection of bacterial chondroitinase ABC in the trunk induces abnormal projections of the ventral motor axons, suggesting the involvement of CS in zebrafish motor axon growth [23]. In vertebrates, the motor axon growth is tightly associated with somite patterning [24]. Generally, each somite has two functionally different components, myotome and sclerotome, giving rise to skeletal muscle of trunk (and tail) and vertebral column respectively. Several lines of evidence suggest the importance of the sclerotomal component in the motor axon guidance in amniotes, whereas that in zebrafish embryos is linked with myotome formation [24]. The reason for such disparity can be explained by the fact that, in contrast with amniote embryos, the zebrafish somite consists predominantly of the myotome, and hence that the sclerotome is a relatively minor component [25]. In addition, the sclerotomal cells in teleosts including zebrafish are believed to differentiate into osteoblasts that produce bone matrix, but not into chondrocytes [26], implying that less cartilaginous anlagen forms in the trunk skeleton during embryogenesis, although cartilaginous skeletons are formed mainly in skull regions during early larval period. These characteristics of the zebrafish embryogenesis would facilitate the exploration of cryptic functions of CS and its biosynthetic enzymes in embryonic developmental processes besides endochondral skeletogenesis, which is severely affected in *C4ST-1*-deficient mice [19]. In the present study, we identified zebrafish *C4ST-1*, and examined its expression and *in vivo* functions during embryogenesis by functional knockdown of the enzyme using specific antisense MOs (morpholino-oligonucleotides).

EXPERIMENTAL

Materials

^{35}S-labelled PAPS (3′-phosphoadenosine 5′-phosphosulfate; 1.35 Ci/mmol) was purchased from PerkinElmer Life Sciences. Unlabelled PAPS was obtained from Sigma. The following sugars and enzymes were purchased from Seikagaku Corporation: chondroitin (a chemically desulfated derivative of whale cartilage CS-A); CS-B (porcine skin DS); six unsaturated standard disaccharides derived from CS {i.e. ΔDi-0S ($\Delta^{4,5}$HexAα1–3GalNAc, where ΔHexA is 4,5-unsaturated hexuronic acid or 4-deoxy-α-L-*threo*-hex-4-enepyranosyluronic acid), ΔDi-6S [$\Delta^{4,5}$HexAα1–3GalNAc(6-*O*-sulfate)], ΔDi-4S [$\Delta^{4,5}$HexAα1–3GalNAc(4-*O*-sulfate)], ΔDi-diS$_D$ [$\Delta^{4,5}$HexA(2-*O*-sulfate)α1–3GalNAc(6-*O*-sulfate), ΔDi-diS$_E$ [$\Delta^{4,5}$HexAα1–3GalNAc(4,6-*O*-disulfate)] and ΔDi-triS [$\Delta^{4,5}$HexA(2-*O*-sulfate)α1–3GalNAc(4,6-*O*-disulfate)]}; conventional chondroitinase ABC (EC 4.2.2.4) from *Proteus vulgaris*; chondroitinase AC-I (EC 4.2.2.5) from *Flavobacterium heparinum*; chondroitinase AC-II (EC 4.2.2.5) from *Arthrobacter aurescens*; and chondroitinase B (EC 4.2.2) from *F. heparinum*. Partially desulfated DS preparations were prepared by solvolysis using porcine skin DS with a high content (approx. 90 %) of 4-O-sulfated disaccharide units [17]. For enzymatic assays of zebrafish sulfotransferases, a partially desulfated DS preparation that contained 4-O-sulfated disaccharide units at 31 % was used, since the preparation has been found to be beneficial for comparative analysis of the substrate preferences of human enzymes, C4ST-1, C4ST-2 and D4ST-1 [17].

Fish maintenance

Zebrafish (*Danio rerio*) embryos were obtained by natural spawning and cultured at 28.5 °C in a 1/3 Ringer solution (39 mM NaCl, 0.97 mM KCl, 0.6 mM $CaCl_2$ and 1.67 mM Hepes, pH 7.2) [27].

Cloning of zebrafish cDNA encoding C4ST-1 and its isoenzymes

A search of the zebrafish EST (expressed sequence tag) database at 'Human BLAST against Zebrafish Shotgun Sequences' using the query sequences of human C4ST-1, C4ST-2, C4ST-3 and D4ST-1 [14–17] retrieved the respective zebrafish 5′- and 3′-ESTs, except for that of C4ST-3, which carried predicted start and stop codons respectively. The cDNAs covering the entire coding regions of the putative zebrafish C4ST-1, C4ST-2 and D4ST-1 were amplified from zebrafish embryonic cDNA by PCR using specific primer sets corresponding to the 5′- and 3′-non-coding regions, based on their respective ESTs. Each amplified cDNA fragment was subcloned into a pGEM®-T Easy vector (Promega) and sequenced in an ABI PRISM™ 377 DNA sequencer (Applied Biosciences). The cDNA sequences have been submitted to the GenBank® Nucleotide Sequence Database with accession numbers AB097217, AB122017 and AB089140 for zebrafish *C4ST-1* (*chst11*), *C4ST-2* (*zC4ST-2*) and *D4ST-1* (*d4st1*) respectively.

Construction of expression vectors encoding soluble forms of zebrafish C4ST-1

The cDNA encoding a truncated form of zebrafish C4ST-1 lacking the first N-terminal 59 amino acid residues was amplified by PCR with the pGEM®-T Easy vector containing the full coding sequence of the protein using a 5′-primer containing an in-frame BamHI site (5′-GCGGATCCCTACAGGAGCTGTAC-3′) and a 3′-primer containing a BamHI site located 19 bp downstream from the stop codon (5′-GCGGATCCCTCAGGAAGCGTGT-3′). PCR was carried out with Pfu DNA polymerase (Promega) by 30 cycles at 95 °C for 42 s, 59 °C for 42 s and 72 °C for 3 min. The PCR products were digested with BamHI, cloned into the BamHI site of an expression vector, pEF-BOS/IP [28], and sequenced. The resultant vector contained cDNA encoding a fusion protein that had an N-terminal cleavable insulin signal peptide and a Protein A IgG-binding domain followed by a truncated form of zebrafish C4ST-1.

Expression and sulfotransferase activity of the soluble forms of recombinant C4ST-1

The expression plasmid (6.7 μg) was transfected into COS-1 cells in 100 mm plates using FuGENE™ 6 transfection reagent (Roche Applied Science) according to the manufacturer's instructions. Two days after transfection, a 1 ml aliquot of the culture medium was incubated with 10 μl of IgG–Sepharose beads (GE Healthcare Bio-Sciences) for 2 h at 4 °C. The enzyme-bound beads were washed with TBS (Tris-buffered saline) containing 0.05 % (w/v) Tween 20, resuspended in the assay buffer described below and subsequently used as enzyme sources for sulfotransferase assays.

Sulfotransferase activities towards chondroitin and partially desulfated DS were assayed as described previously [17]. Briefly, the standard mixture (60 μl) contained 10 μl of the resuspended beads, 50 mM imidazole/HCl (pH 6.8), 2 mM dithiothreitol, 10 μM [^{35}S]PAPS (1 or 3×10^5 d.p.m.) and chondroitin or partially desulfated DS (10 nmol as GlcA) as an acceptor. The reaction mixtures were incubated at 28 °C for 30 or 60 min and subjected to gel filtration using a syringe column packed with Sephadex G-25 (superfine). The incorporation of [^{35}S]sulfate into chondroitin or partially desulfated DS was quantified by determination of the radioactivity in the flow-through fractions by liquid-scintillation counting. For identification of the transferase reaction products, the radioactive flow-through fractions were individually subjected to exhaustive digestion with chondroitinase ABC, AC-I or B. Each digest was analysed by anion-exchange HPLC on an amine-bound silica PA-03 column (YMC).

Whole-mount *in situ* hybridization

Digoxigenin-labelled RNA probes were transcribed *in vitro* using T7 or SP6 RNA polymerase, with the linearized pGEM®-T EASY vector containing the full-length cDNA of zebrafish *C4ST-1* (approx. 1.2 kb). Other probes for *shha* (*sonic hedgehog*; UniGene Cluster Dr.36074) [29] and *myod* (*myogenic differentiation*; UniGene Cluster Dr.36017) [30] were also synthesized. These cDNA fragments were amplified by PCR using embryonic zebrafish cDNA. For a cDNA fragment (approx. 700 bp) of zebrafish *shha*, the first PCR was performed with 5′-TTCGGCTCTGGTCTCGCTCCA-3′ as a forward primer, 5′-ATATCCCAACTCGCTCGAGCC-3′ as a reverse primer, and followed by nested PCR with 5′-GGAGGACAGAAGGCCGTGAAG-3′ and 5′-CTCTCACTCTCGCTCTCTCTC-3′. A cDNA fragment (approx. 640 bp) of zebrafish *myod* was amplified with 5′-CGAGCATCACCACATCGAGGA-3′ and 5′-TCGTTTAAGGTCGGATTCGCC-3′, followed by nested PCR with 5′-AGCACGTGAGGGCGCCCAGTG-3′ and 5′-CCTGAGCCTGCTGTTGAGGGC-3′. Each fragment was subcloned into a pGEM®-T EASY vector and the resultant plasmids were used as a template for the synthesis of the riboprobes.

Whole-mount *in situ* hybridization was carried out as described previously [31] with slight modifications. Zebrafish embryos were permeabilized by treatment with proteinase K (10 μg/ml), and then fixed with 4 % (w/v) PFA (paraformaldehyde)/PBS. The embryos were then treated with a hybridization buffer [50 % (v/v) formamide, 5× SSC (1× SSC is 0.15 M NaCl/0.015 M sodium citrate), 0.1 % (w/v) Tween 20, 50 μg/ml tRNA, 0.1 mg/ml single-stranded DNA and 50 μg/ml Hep] at 55 °C for 4 h, followed by hybridization with the appropriate digoxigenin-labelled RNA probe at 55 °C for 16 h. Thereafter, the embryos were treated with RNase A at 37 °C for 1 h in order to remove the excess probes; immersed in a blocking solution [150 mM maleate, 100 mM NaCl, 0.1 % (w/v) Tween 20 and 2 % (w/v) blocking reagent (Roche Applied Science), pH 7.5] at 4 °C for 4 h; incubated with anti-digoxigenin antibody conjugated with alkaline phosphatase (Roche) diluted 1:5000 with the blocking solution at room temperature (25 °C) for 4 h; and stained with an alkaline phosphatase substrate, BM Purple (Roche). The stained embryos were postfixed with 4 % PFA/PBS at room temperature for 30 min and then soaked in 50 % (w/v) glycerol/PBS overnight at 4 °C. Images were obtained using stereoscopic (SZX12) and confocal (BX51) microscopes (Olympus) equipped with a digital camera (CX380; Olympus).

Gene knockdown by morpholinos

MOs directed against *C4ST-1* were synthesized by Gene-Tools (Figure 4). The sequences of the MOs used are as follows: MO1, the sequence (25 bases) of which corresponds to that around the start codon, 5′-GGTCCAGTATGGTTTGTTTCATGGC-3′; control MO with five-base-mismatched nucleotides compared with MO1 (5-mis MO1), 5′-GGTaCAcTATGcTTTcTTTCATcGC-3′; control MO with the inverted sequence of MO1 (inverted MO1), 5′-CGGTACTTTGTTTGGTATGACCTGG-3′; MO2, the sequence (25 bases) of which corresponds to the 5′-non-coding region (–56 to –32), 5′-CTGCCGAGCCGAGCCCCGTTCAGCG-3′. Each MO was dissolved in distilled water at a final concentration of 8 mM. The stock solution was diluted to a working concentration of 0.8 mM in 1× Danieau solution (58 mM NaCl, 0.7 mM KCl, 0.4 mM $MgSO_4$, 0.6 mM $CaCl_2$ and 5 mM Hepes, pH 7.6), optionally with a non-toxic tracer, rhodamine–dextran (Molecular Probes) [32].

Each MO (approx. 3–5 ng) was individually injected into two- or four-cell embryos. MO-injected embryos (morphants) were incubated in a 1/3 Ringer solution containing 1 % penicillin/streptomycin at 28.5 °C for 16–50 h.

Inhibitory effects of the MOs on *in vitro* translation of zebrafish C4ST-1

For the preparation of mRNA, Myc-tagged sulfotransferase constructs were generated by in-frame insertion of the cDNA fragment of zebrafish *C4ST-1*, *C4ST-2* or *D4ST-1* into a pcDNA3.1/myc-His (–) vector (Invitrogen), and subsequently subcloned into a pEU3-NII vector (Toyobo). mRNAs encoding the fusion proteins with a C-terminal Myc tag were transcribed *in vitro* using ScriptMAX™ (Toyobo) with each pEU3-NII vector construct as a template. *In vitro* translation in the presence or absence of MOs was performed by using a cell-free protein synthesis kit, PROTEIOS™ (Toyobo), with the following modifications: in a 25 μl reaction, the transcribed mRNA (7 μg) and each MO at a final concentration of 100 μM were mixed with a reaction mixture containing components essential for *in vitro* translation and incubated at 26 °C for 24 h. An aliquot of the reaction mixture was heated at 95 °C for 5 min and then subjected to SDS/PAGE and proteins were transferred to a PVDF membrane. After pretreatment with a blocking solution [PBS containing 0.05 % (w/v) Tween 20 and 5 % (w/v) ECL® advance blocking reagent (GE Healthcare Bio-Sciences)], the membrane was treated with an anti-Myc antibody (Invitrogen), and subsequently with a horseradish peroxidase-conjugated anti-mouse IgG (GE Healthcare Bio-Sciences). Proteins bound to the antibody were visualized with an ECL® advance kit (GE Healthcare Bio-Sciences).

Rescue of morphological phenotypes of the MO1-injected embryos by injection with zebrafish *C4ST-1* RNA

A capped zebrafish *C4ST-1* sense RNA was synthesized using an mMASSAGE mMACHINE kit (Ambion) according to the manufacturer's protocol from a linearized pCS2+ vector carrying

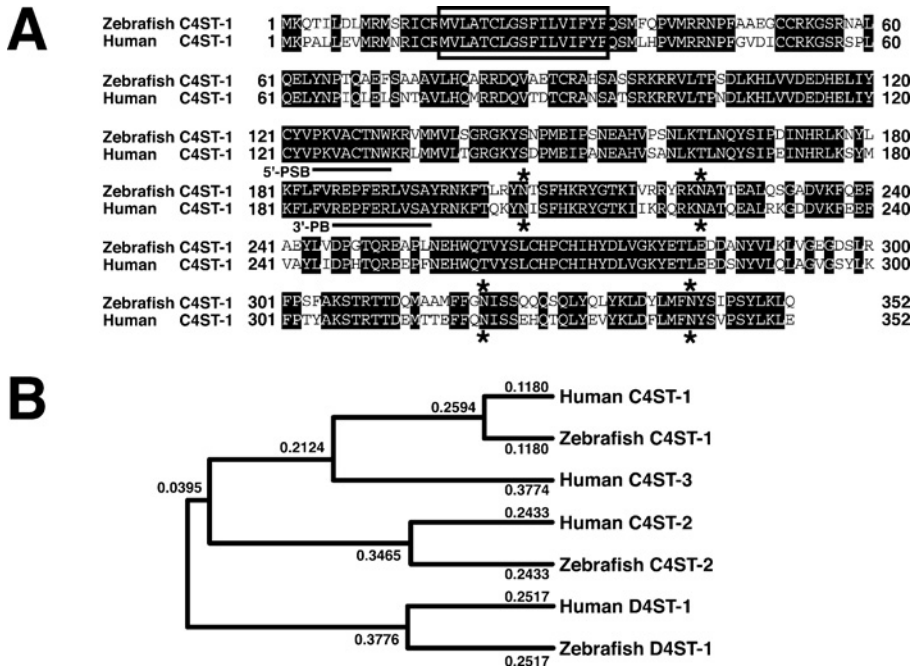

Figure 1 Comparison of the amino acid sequences of zebrafish and human C4ST-1 (A) and phylogenetic relations of subfamily members (B)

(**A**) Alignment of zebrafish and human C4ST-1 was performed using GENETYX-MAC (version 10.1) software. The aligned amino acids are shaded black if identical. The single transmembrane domain and potential N-linked glycosylation sites are indicated by a square box and asterisks respectively. Putative binding sites for the 5′-phosphosulfate group (5′-PSB) and 3′-phosphate group (3′-PB) of PAPS are underlined. (**B**) Apparent evolutional relationships of zebrafish and human C4ST/D4ST subfamily members were examined using GENETYX-MAC software. The length of each horizontal line is proportional to the degree of the divergence of the amino acid sequence.

the entire coding region of zebrafish *C4ST-1*. Zebrafish *C4ST-1* sense RNA (4–6 pg) was injected separately, immediately after the injection of MO1 into two-cell embryos.

Disaccharide composition analysis

GAG peptides derived from zebrafish embryos were prepared as described previously [33] but with minor modifications: dechorionated wild-type and MO1-treated embryos at 50 hpf (hours post fertilization) (approx. 160 and 300 embryos respectively) were homogenized in acetone and air-dried. The dried materials (9 and 16 mg respectively) were treated with boiling water for 10 min, cooled and exhaustively digested with heat-pretreated actinase E in 1 ml of 0.1 M borate buffer (pH 8.0), containing 10 mM calcium chloride at 60 °C for 16 h. The digest was treated with 5 % (v/v) trichloroacetic acid, and the acid-soluble fraction was extracted with diethyl ether. The aqueous phase was neutralized with 1 M sodium carbonate and adjusted to contain 80 % ethanol. The resultant precipitate was dissolved in water and subjected to gel filtration on a PD-10 column (GE Healthcare Bio-Sciences) with 50 mM pyridine acetate (pH 5.0) as eluent. The flow-through fractions were collected, evaporated dry and dissolved in water. An aliquot of the sample was digested with a mixture of chondroitinases ABC and AC-II in 50 mM Tris/HCl and 60 mM sodium acetate (pH 8.0) at 37 °C for 2 h. The digests were derivatized with a fluorophore, 2-AB (2-aminobenzamide), and then analysed by anion-exchange HPLC on a PA-03 column [34].

Immunohistochemistry

Wild-type and MO1-treated embryos (48–51 hpf) were fixed in 4 % PFA/PBS, dehydrated through graded concentrations of methanol and stored in methanol at − 20 °C until used. The embryos were rehydrated in a stepwise fashion through a PBS-T (PBS containing 0.1 % Tween 20)/methanol series. After rinsing in PBS-T, the embryos were treated sequentially with the following solutions: (i) 3 % (w/v) H_2O_2 in methanol for 5 min; (ii) proteinase K (10 μg/ml) in PBS at 37 °C for 60 min; (iii) 4 % PFA/PBS for 20 min for postfixation; (iv) pre-chilled acetone at − 20 °C for 8 min; (v) the above-mentioned blocking solution at 4 °C for 2 h; (vi) anti-acetylated α-tubulin (1:100, clone 6-11B-1; Sigma) in the blocking solution overnight at 4 °C; (vii) horseradish peroxidase-conjugated anti-mouse IgG (1:200) in the blocking solution overnight at 4 °C; (viii) 0.05 % DAB (diaminobenzidine) in PBS for 20 min; and (ix) 0.01 % DAB/3 % H_2O_2 in PBS for 5–15 min. Finally, the embryos were fixed with 4 % PFA/PBS and then soaked in 50 % glycerol/PBS.

RESULTS

Identification of zebrafish C4ST-1 and its isoenzymes

Our preliminary analysis of the disaccharide composition of CS present in the zebrafish embryos revealed that the 4-O-sulfation of GalNAc was a prominent modification of CS in the embryos as well as in the adult fish as recently reported [35]. In support of the prior analyses, a search of the zebrafish EST database showed the existence of at least three distinct zebrafish GalNAc 4-*O*-sulfotransferases potentially responsible for the 4-O-sulfation of CS/DS. Predicted open reading frames of the candidate enzymes were amplified by PCR using primers designed from the retrieved ESTs and the cDNA library of the 24-hpf zebrafish embryo as a template. One of the cDNA fragments (GenBank® accession number AB097217) obtained encoded a protein of 352 amino acid residues with a transmembrane domain, the putative PAPS-binding motifs, and 79 % identity to human C4ST-1 [14] at the amino acid level (Figure 1A). The deduced amino acid

Table 1 Comparison of the acceptor specificity of zebrafish and human C4ST-1

The recombinant zebrafish and human C4ST-1 were assayed using chondroitin and partially desulfated DS as acceptors (10 nmol as GlcA) as described in the Experimental section. The reaction products were separated from [^{35}S]PAPS by gel filtration on a syringe column packed with Sephadex G-25 (superfine). The radioactivity was measured by using liquid-scintillation counting.

	C4ST-1*† (pmol per ml of medium/h)	
Acceptor	Zebrafish	Human‡
Chondroitin	489	609
Partially desulfated DS	330	206

*The values represent the averages for two independent experiments.

†No detectable sulfotransferase activity was detected towards chondroitin or partially desulfated DS when the medium from cells transfected with the empty vector was used as an enzyme source in the control experiment.

‡The sulfotransferase activity of human C4ST-1 in [17].

sequences of the other two cDNAs (GenBank® accession numbers AB122017 and AB089140) had 61 and 65 % identity to human C4ST-2 [14] and D4ST-1 [16,17] respectively. Phylogenetic analysis indicated that each zebrafish protein could be assigned to one of the human C4ST/D4ST subfamily members, except for C4ST-3 [15,17] (Figure 1B). Consequently, the zebrafish gene products of AB097217, AB122017 and AB089140 were named zebrafish C4ST-1, C4ST-2 and D4ST-1 respectively.

Characterization of zebrafish C4ST-1

To assess the sulfotransferase activity of zebrafish C4ST-1, a soluble form of the protein was generated by replacing the first 59 amino acids with a cleavable insulin signal sequence and a Protein A IgG-binding domain as described in the Experimental section, and then the chimaeric proteins were transiently expressed in COS-1 cells. The recombinant enzyme secreted into the culture medium was absorbed to IgG–Sepharose beads to eliminate endogenous sulfotransferase activities, and then the enzyme-bound beads were used for the enzyme assays. As shown in Table 1, the recombinant zebrafish C4ST-1 transferred [^{35}S]sulfate from [^{35}S]PAPS to both chondroitin and partially desulfated DS (containing 4-O-sulfated units at 31 %) with approx. 1.5-fold greater incorporation into the former than into the latter. It should be noted that the partially desulfated DS used has been previously shown to be an excellent acceptor comparable with exhaustively desulfated DS under our assay conditions [17]. This substrate preference of the zebrafish enzyme was quite similar to that of human C4ST-1.

In order to identify the reaction products, the ^{35}S-labelled products were digested exhaustively with chondroitinase ABC, which cleaves both the GalNAc–GlcA and GalNAc–IdoA linkages in CS/DS, and then the digests were analysed by anion-exchange HPLC. In both digests of the reaction products, which were obtained by using chondroitin (Figure 2A) or partially desulfated DS (results not shown) as an acceptor, almost all of the total radioactivity was recovered at the elution position corresponding to the unsaturated disaccharide ΔDi-4S [ΔHexA-GalNAc(4S)], demonstrating that zebrafish C4ST-1 indeed catalysed the 4-O-sulfation of GalNAc residues in these polymers.

To further characterize the acceptor specificity of zebrafish C4ST-1, the radiolabelled 4-O-sulfation sites in the reaction products, which were obtained by incubation of C4ST-1 with

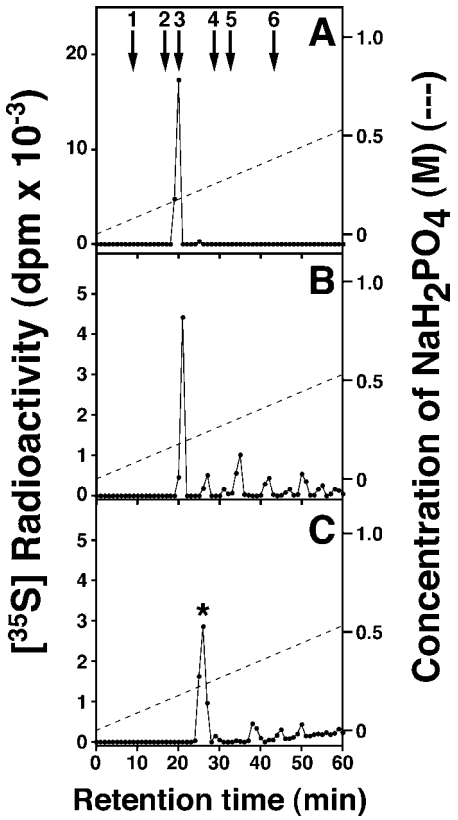

Figure 2 Identification of the zebrafish C4ST-1 reaction products prepared using chondroitin or partially desulfated DS as the acceptor substrate

^{35}S-labelled zebrafish C4ST-1 reaction products, which were obtained by using chondroitin (**A**) or partially desulfated DS (**B**, **C**) as the sulfate acceptor, were digested with chondroitinase ABC (**A**), chondroitinase AC-I (**B**) or chondroitinase B (**C**). Each digest was analysed by anion-exchange HPLC on an amine-bound silica PA-03 column using a linear gradient of NaH_2PO_4 from 16 to 530 mM over a 60 min period. The major radioactive peak marked by an asterisk in (**C**) is the putative monosulfated tetrasaccharide(s) identified previously [17]. The arrows indicate the elution positions of authentic unsaturated disaccharides: 1, ΔDi-0S; 2, ΔDi-6S; 3, ΔDi-4S; 4, ΔDi-diS_D; 5, ΔDi-diS_E; 6, ΔDi-triS.

partially desulfated DS, were structurally analysed, because porcine DS contains not only a large proportion of IdoA but also a very small proportion of GlcA. To this end, the reaction products were exhaustively digested with chondroitinase AC-I or chondroitinase B, which cleaves the GalNAc–GlcA linkages or GalNAc–IdoA linkages in CS/DS respectively. As reported previously [17], the ^{35}S-labelled DS preparations treated with the individual chondroitinases were decomposed into radioactive di-, tetra-, hexa-, octa- and higher oligosaccharides, depending on the distribution of GalNAc–GlcA/IdoA linkages in the polymer (results not shown). Particularly, quantification of the radio-labelled, 4-O-sulfated disaccharides derived from each digest provided important information regarding the preferable sequences (i.e. GalNAc residues flanked by either GlcA or IdoA) recognized by zebrafish C4ST-1. In the analysis of the radiolabelled reaction product of zebrafish C4ST-1, as much as 23 % of total radioactivity was identified as ΔDi-4S in the chondroitinase AC-I digest (Figure 2B), whereas negligible radioactivity was detected at the position of ΔDi-4S in the chondroitinase B digest (Figure 2C), suggesting the strong preference of zebrafish C4ST-1 for the sequence -GlcA-GalNAc(4S)-GlcA- over -IdoA-GalNAc(4S)-IdoA-, this being consistent with the marked preference of human C4ST-1

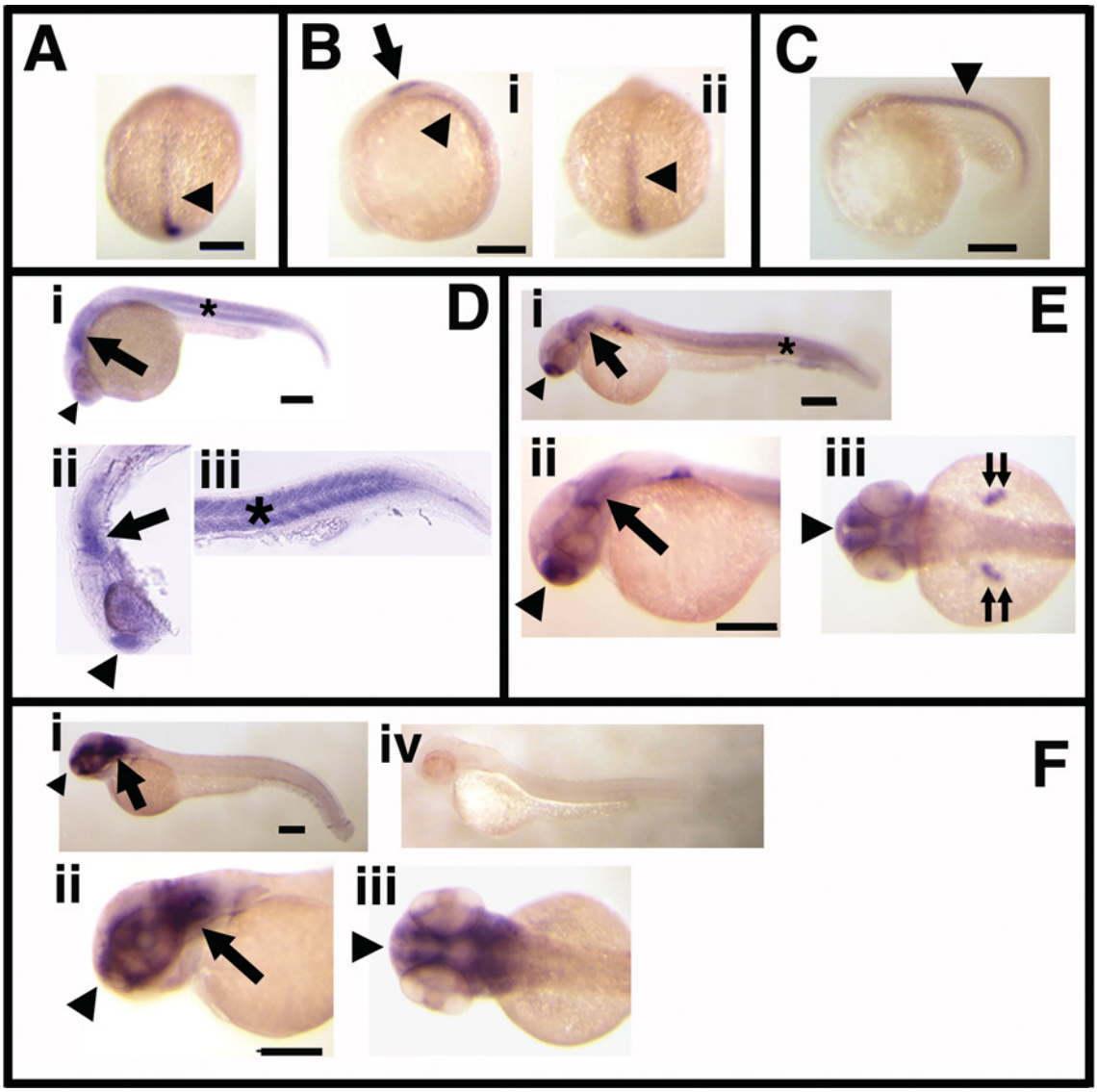

Figure 3 Expression of *C4ST-1* mRNA in zebrafish embryos

Expression of *C4ST-1* in zebrafish embryos at 10.5 (**A**), 13 (**B**), 18 (**C**), 24 (**D**), 36 (**E**) and 48 hpf (**F**). (**A**–**C**) *C4ST-1* was expressed in the notochord (arrowhead) and the spinal cord (arrow). (**D**, **E**) At 24 and 36 hpf, the expression was also observed in the somite (asterisk), the telencephalon (arrowhead), the rhombencephalon (arrow) and the pectoral fin buds (double arrows). Panels (**ii**) and (**iii**) of (**B**–**F**) are magnified images of the respective panels (**i**). (**F**) *C4ST-1* transcript was expressed in the telencephalon (arrowhead) and the rhombencephalon (arrow) at 48 hpf. No signal was detected by using a sense probe for *C4ST-1* [**F**(**iv**)]. [**A**, **B**(**ii**)] Dorsal view, anterior to the top. [**E**(**iii**), **F**(**iii**)] Dorsal view, anterior to the left. [**B**(**i**), **C**, **D**, **E**(**i**), **E**(**ii**), **F**(**i**), **F**(**ii**), **F**(**iv**)] Lateral view, anterior to the left. Scale bars, 200 μm.

for GalNAc residues in the GlcA-rich regions embedded in CS/DS [17]. We also detected GalNAc 4-*O*-sulfotransferase activities of zebrafish C4ST-2 and D4ST-1 towards chondroitin and partially desulfated DS. In terms of the preference for the isomeric uronic acids flanking the target GalNAc residues, their characteristics also closely resembled those of the respective human counterparts [17]: zebrafish D4ST-1 showed the opposite preference to zebrafish C4ST-1, and zebrafish C4ST-2 exhibited a less stringent structural requirement (results not shown). Taken together, the enzymatic specificities of these zebrafish enzymes strongly support orthologous relationships with their respective human counterparts (Figure 1B).

Because of an apparent predominance of C4ST-1 in CS biosynthesis and embryogenesis in mammals [18,19], compared with the other subfamily members, we focused on the biological functions of zebrafish C4ST-1 in the present study.

Expression pattern of C4ST-1 in zebrafish embryos

The developmental expression pattern of zebrafish *C4ST-1* was examined by whole-mount *in situ* hybridization using the specific antisense probe labelled with a digoxigenin. *C4ST-1* was detected in the notochord at 10.5–18 hpf within the segmentation period (Figures 3A–3C). A transient expression was also observed in the spinal cord at 13 hpf (Figure 3B). At 24 hpf, *C4ST-1* was strongly expressed in the somite, telencephalon and rhombencephalon, and the expression in the somite and brain persisted through 36 and 48 hpf respectively [Figures 3D, 3E and 3F(i–iii)]. In addition, the *C4ST-1* transcript was also transiently expressed in the fin buds at 36 hpf (Figure 3E). The sense probe for *C4ST-1* gave no signal throughout the entire embryo during all stages analysed [Figure 3F(iv) and results not shown], confirming the specific hybridization of the antisense probe.

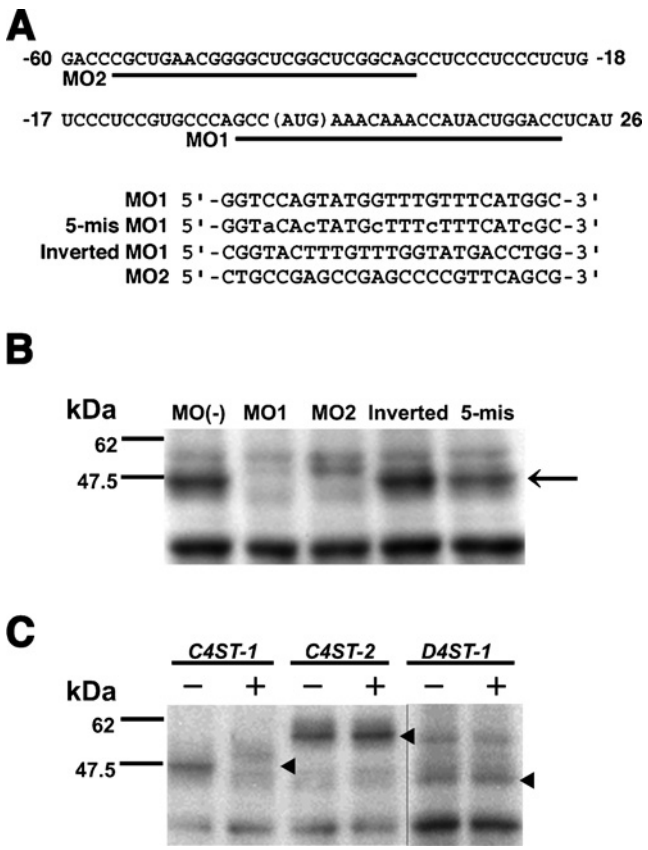

Figure 4 MOs directed against *C4ST-1* and their inhibitory effects on *in vitro* translation of *C4ST-1*

(**A**) *C4ST-1*-specific MOs, MO1 and MO2, were synthesized based on the nucleotide sequence of *C4ST-1* mRNA in the vicinity of the start codon (given in parentheses). 5-Mis MO1 and inverted MO1 were used as negative controls. The former has five-base-mismatched nucleotides compared with MO1 (indicated by lower-case letters), and the latter has the inverted sequence of MO1. (**B**) mRNA encoding C4ST-1/Myc was translated *in vitro* in the absence (–) or presence of each MO. (**C**) mRNAs encoding C4ST-1/Myc, C4ST-2/Myc and D4ST-1/Myc were individually translated *in vitro* in the absence (–) or presence (+) of MO1. The translated Myc-tagged proteins were analysed by Western blotting using an anti-Myc antibody (**B**, **C**). An arrow in (**B**) and arrowheads in (**C**) indicate the positions of C4ST-1/Myc and each Myc-tagged protein respectively. Bars on the left in (**B**) and (**C**) indicate the positions of standard protein markers.

Specificity of antisense MOs

The injection of antisense MOs has been demonstrated to inhibit the target gene functions in zebrafish embryos [32]. For functional knockdown of *C4ST-1*, we designed *C4ST-1*-specific MOs (MO1 and MO2) and control MOs (5-mis MO1 and inverted MO1) based on the nucleotide sequence of zebrafish *C4ST-1* mRNA in the vicinity of the start codon (Figure 4A and see the Experimental section). The specificity of the MOs was verified by an *in vitro* translational inhibition assay using a cell-free protein synthesis system. Incubation with MO1 or MO2 efficiently inhibited the translation of C4ST-1–Myc fusion protein, whereas no inhibitory effects were observed in the reaction mixture containing the individual control MOs (Figure 4B). In addition, MO1 did not interfere with the translation of the fusion proteins of C4ST-2 and D4ST-1 (Figure 4C).

Inhibition of C4ST-1 function causes morphological abnormalities in the trunk and tail

In order to assess the biological roles of 4-O-sulfated CS during zebrafish embryogenesis, *C4ST-1*-specific MOs and control MOs were individually injected into one- to four-cell stage embryos. The 48 hpf embryos injected with MO1 (approx. 3–5 ng per embryo) displayed a ventrally bent trunk and a curled and/or kinky tail (Figures 5B and 5B′). Furthermore, the injection of MO1 at higher dosages (> 5 ng per embryo) resulted in embryonic lethality by 48 hpf, and most of the embryos exhibited a severely shrunken body (Figure 5D). Thus, to avoid any non-specific toxicity of MOs, subsequent injections were conducted at dosages of 3–5 ng of MO per embryo. The morphological phenotypes of MO2-injected embryos were also similar to those of MO1-injected embryos (Figures 5C and 5C′), although the potential for functional knockdown of *C4ST-1* appeared to be less than that of MO1 (Figure 5H). In contrast, most of the embryos injected with control MOs, 5-mis or inverted MO1 developed normally (Figures 5E, 5F and 5H) as did wild-type embryos (Figures 5A and 5A′). In addition, co-injection of a zebrafish *C4ST-1* RNA (4–6 pg per embryo; $n = 20/31$, 64.5 %; $P < 0.001$, χ^2 test) definitely rescued the morphological phenotypes of MO1-injected embryos (Figure 5G). These findings suggest that the morphological abnormalities in the body axis are caused by functional knockdown of *C4ST-1*, not by non-specific toxicity of MOs.

Analysis of CS of C4ST-1 morphants

To further verify the specificity of *C4ST-1*-specific MOs *in vivo*, GAG fractions prepared from wild-type and MO1-injected embryos at 50 hpf were chemically analysed. For exhaustive digestion of CS moieties, the purified GAG-peptide was treated with a mixture of chondroitinases ABC and AC-II. The resultant unsaturated CS disaccharides were derivatized with a fluorophore, 2-AB, followed by anion-exchange HPLC on a PA-03 column. As shown in Figure 6(A), in wild-type embryos, ΔDi-4S was the predominant sulfated disaccharide, accounting for 36.6 % of all the disaccharides of CS (Table 2). As expected, the amount of ΔDi-4S in MO1-injected embryos was reduced by approximately one-third (Figure 6B and Table 2), suggesting a selective inhibitory effect of MO1 on the C4ST-1-mediated sulfation *in vivo*. Notably, the amount of CS (total disaccharides) in MO1-injected embryos was also approximately half that in wild-type embryos, due to significant reductions in non-sulfated disaccharide (ΔDi-0S) in addition to ΔDi-4S (Table 2). Together with previous biochemical analyses of CS in sog9 cells and in the growth plates of *C4ST-1*-deficient mice [18,19], these results indicate that C4ST-1 may also regulate the amount of CS, in addition to the 4-O-sulfation.

C4ST-1 is required for normal somite formation

Strong expression of *C4ST-1* in the notochord and somites (Figures 3A–3E), which are major components of the body axis during embryogenesis, indicated the aberrant morphology of the body axis observed in *C4ST-1* morphants to be caused by defects in the notochord and/or somites. To address this issue, we examined expression of the marker genes, *shha* [29] and *myod* [30], involved in the development of the notochord and skeletal muscle respectively, because zebrafish somites are almost exclusively occupied by myotomes, which give rise to the axial musculature through regulation of myogenic transcription factors including myoD [25,30]. In *C4ST-1* morphants, the signal of *shha* was observed along a rostrocaudal axis with a pattern of expression that was virtually the same as in wild-type embryos (Figures 7A and 7B) [29,36]. The profile of *myod* expression in the morphants at 16 hpf was also essentially indistinguishable from that in wild-type embryos, except that the expression in the morphants was expanded laterally to some extent (Figures 7C and 7D). Intriguingly, at 30 hpf, when development progressed

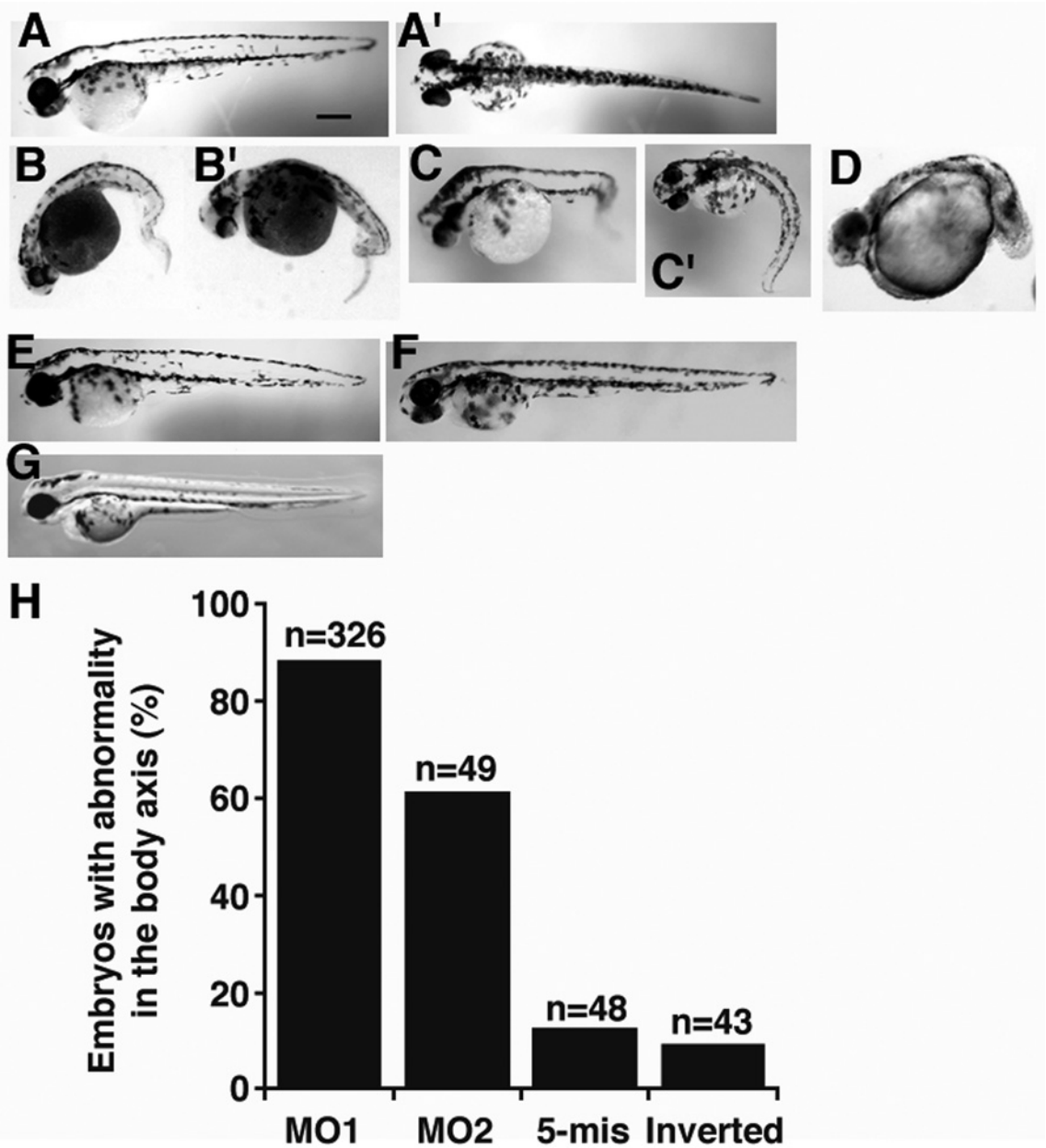

Figure 5 Morphological abnormality in *C4ST-1* morphants

(**A**, **A′**) A 48 hpf wild-type embryo. (**B**, **B′**, **C**, **C′**) Representative morphologies of 48 hpf embryos injected with 3–5 ng of MO1 (**B**, **B′**) or MO2 (**C**, **C′**). They had a ventrally bent trunk and a curled and/or kinky tail. (**D**) Injection of >5 ng of MO1 was embryonic lethal by 48 hpf, and the morphology of the embryos was characterized by a severely shrunken body. (**E**, **F**) Embryos injected with 3–5 ng of 5-mis MO1 (**E**) or inverted MO1 (**F**) showed no obvious abnormality. (**G**) The morphological phenotypes of MO1-injected embryos were definitely rescued by injection with zebrafish *C4ST-1* RNA (4–6 pg per embryo). (**H**) Incidence of 48 hpf embryos with morphological abnormalities in the body axis after injection of each MO (3–5 ng). *n* represents the number of embryos injected with each MO. (**A**–**G**) Lateral view, anterior to the left. (**A′**, **B′**, **C′**) Dorsal view, anterior to the left.

further, *myod* in the somites disappeared in wild-type embryos (Figure 7E), whereas the high level of expression persisted in the *C4ST-1* morphants (Figure 7F). These observations suggest that the aberrant morphology in *C4ST-1* morphants is largely due to perturbation of somitic muscle development and not to notochordal defects.

Involvement of 4-O-sulfated CS in the motor axon guidance

A previous report by Bernhardt and Schachner [23] has suggested that CS has regulatory roles in axon guidance for ventral motor nerves in zebrafish embryos. This prompted us to investigate the overall pattern of the axonal projections from motor neurons in the *C4ST-1* morphants. Therefore, to visualize the ventral motor axons, 48–51 hpf MO1-treated and wild-type embryos were immunostained with anti-acetylated α-tubulin. As shown in Figures 7(G) and 7(I), the wild-type embryos exhibited regularly spaced, stereotyped ventral trajectories of motor axons along the midsegmental region of each somite. Since the segmentation process appeared morphologically normal in the *C4ST-1* morphants, the spatial arrangement of individual axons was almost identical with that in the wild-type embryos

Table 2 Disaccharide composition of CS from 50 hpf wild-type embryos and *C4ST-1* morphants

n.d., not detected.

	Wild-type embryos [pmol/mg of acetone powder (mol%)]	*C4ST-1* morphants [pmol/mg of acetone powder (mol%)]
ΔDi-0S	113.3 (53.6)	66.5 (58.4)
ΔDi-6S	17.9 (8.5)	16.7 (14.7)
ΔDi-4S	77.4 (36.6)	28.8 (25.3)
ΔDi-diS_D	2.9 (1.4)	1.9 (1.7)
ΔDi-diS_E	n.d.	n.d.
ΔDi-triS	n.d.	n.d.
Total CS/DS	211.5	113.9

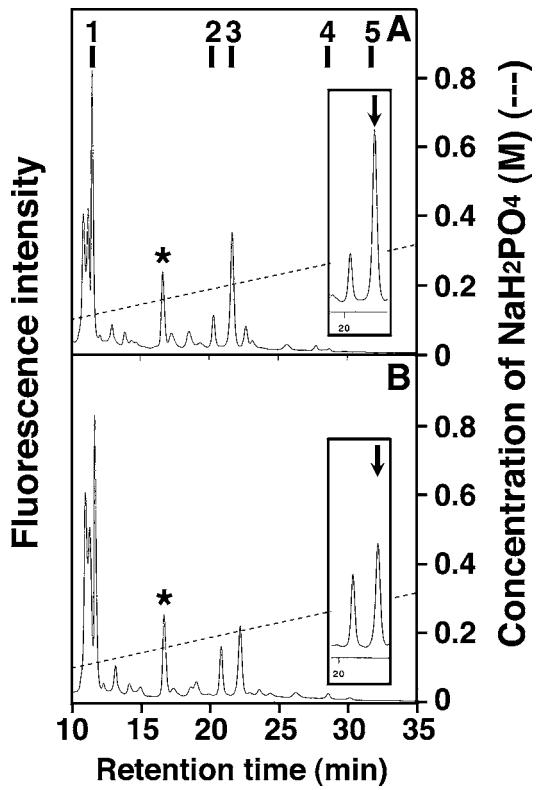

Figure 6 Anion-exchange HPLC analysis of CS derived from 50 hpf wild-type embryos and *C4ST-1* morphants

The GAG preparations purified from pooled 50 hpf wild-type embryos (**A**) and the *C4ST-1* morphants (**B**) were digested with a mixture of chondroitinases ABC and AC-II. The individual digests were labelled with the fluorophore 2-AB and analysed by anion-exchange HPLC as described in the legend of Figure 2. Insets of (**A**) and (**B**) are magnified chromatograms around the elution position corresponding to ΔDi-4S-2-AB (indicated by an arrow). Notably, the fluorescence intensity corresponding to the 4-O-sulfated disaccharide was significantly reduced in the *C4ST-1* morphants compared with the wild-type embryos. Vertical lines indicate the elution positions of 2-AB labelled, authentic unsaturated disaccharides: 1, ΔDi-0S-2-AB; 2, ΔDi-6S-2-AB; 3, ΔDi-4S-2-AB; 4, ΔDi-diS_D-2-AB; 5, ΔDi-diS_E-2-AB. The peaks marked by asterisks in (**A**) and (**B**) are unidentified materials.

(Figures 7H and 7J). However, many of the *C4ST-1* morphants had truncated, abnormally branched and/or misrouted axons (Figures 7H and 7J). Clearly recognizable ventral motor axons in the trunk and tail regions of these embryos were categorized into three groups by their morphological criteria (Table 3). Truncation and abnormal branching occurred significantly more often in the *C4ST-1* morphants than in the wild-type embryos. It should be noted that the axons observed in the morphants with a sharply bent trunk and/or a highly twisted tail were not scored for this classification to exclude the possibility that aberrant projections were caused by mechanical distortion of their profoundly altered body shapes. These results provide the first direct genetic evidence for the involvement of 4-O-sulfated CS in the axon guidance of ventral motor nerves.

Table 3 Incidence of abnormal motor axons in 48–51 hpf wild-type embryos and *C4ST-1* morphants

Ventral motor axons on only one body side per embryo were scored. Note that the aberrant axons in *C4ST-1* morphants with a sharply bent trunk and/or a highly twisted tail were not scored to exclude undesirable effects on axonal growth by mechanical distortion of their profoundly altered body shapes. The significance of wild-type embryos compared with *C4ST-1* morphants for each criterion was determined by a χ^2 test.

		n (% of total)		
	Nerves scored (total)	Truncation	Branching	Aberrant directions
Wild-type	162	3 (1.9)	0	0
C4ST-1 morphants	254	97 (38.2)*	11 (4.3)†	5 (2.0)‡

*$P < 0.001$.
†$P < 0.01$.
‡Not significant.

DISCUSSION

In the present study, a morpholino-based knockdown of zebrafish *C4ST-1*, whose product catalysed preferentially 4-O-sulfation of GalNAc residues in CS, was conducted to clarify the biological roles of CS in vertebrate embryogenesis. Biochemical analysis of CS derived from the *C4ST-1* morphants revealed that the enzyme is essential not only for 4-O-sulfation of CS but also for regulation of the amount of CS *in vivo*. In addition, the *C4ST-1* morphants displayed abnormal morphologies in the trunk and tail with perturbed expression of a myogenic marker *myod*, and in the projections of the ventral motor axons, providing the first genetic evidence for novel functions of 4-O-sulfated CS formed by C4ST-1 in skeletal muscle development and axon guidance during zebrafish embryogenesis.

As in mammals, the 4-O-sulfated structure was the predominant modification of CS in zebrafish embryos (Table 2). In addition, the existence of the sulfation machinery constituted by C4ST-1, C4ST-2 and D4ST-1 in zebrafish (Figure 1), and the strict substrate preferences towards chondroitin and partially desulfated DS (Figure 2 and Table 1), which were almost equivalent to those of the respective human counterparts [17], permitted the investigation of functions of these enzymes both in CS biosynthesis and in embryonic development using this representative model animal. It was recently reported that a single deficiency of *C4ST-1* in sog9 cells and a gene-trapped mutant mouse led to extensively reduced productivity in terms of the 4-O-sulfation and amount of CS [18,19]. Consistent with these observations, functional knockdown of *C4ST-1* in zebrafish embryos also resulted in a reduction in the 4-O-sulfation and amount of CS (Table 2), although the rate of decrease was milder with a MO-based knockdown than in sog9 cells and *C4ST-1*-deficient mice. This is probably attributable to the less severe penetrance in the phenotypes elicited by treatment with the *C4ST-1*-specific MO rather than to functional compensation by C4ST-2 and/or D4ST-1, because we used pooled MO1-treated embryos showing a mild phenotype in the body axis for the biochemical analysis of CS to avoid non-specific side effects of MO. Furthermore, an analysis using an *in vitro*

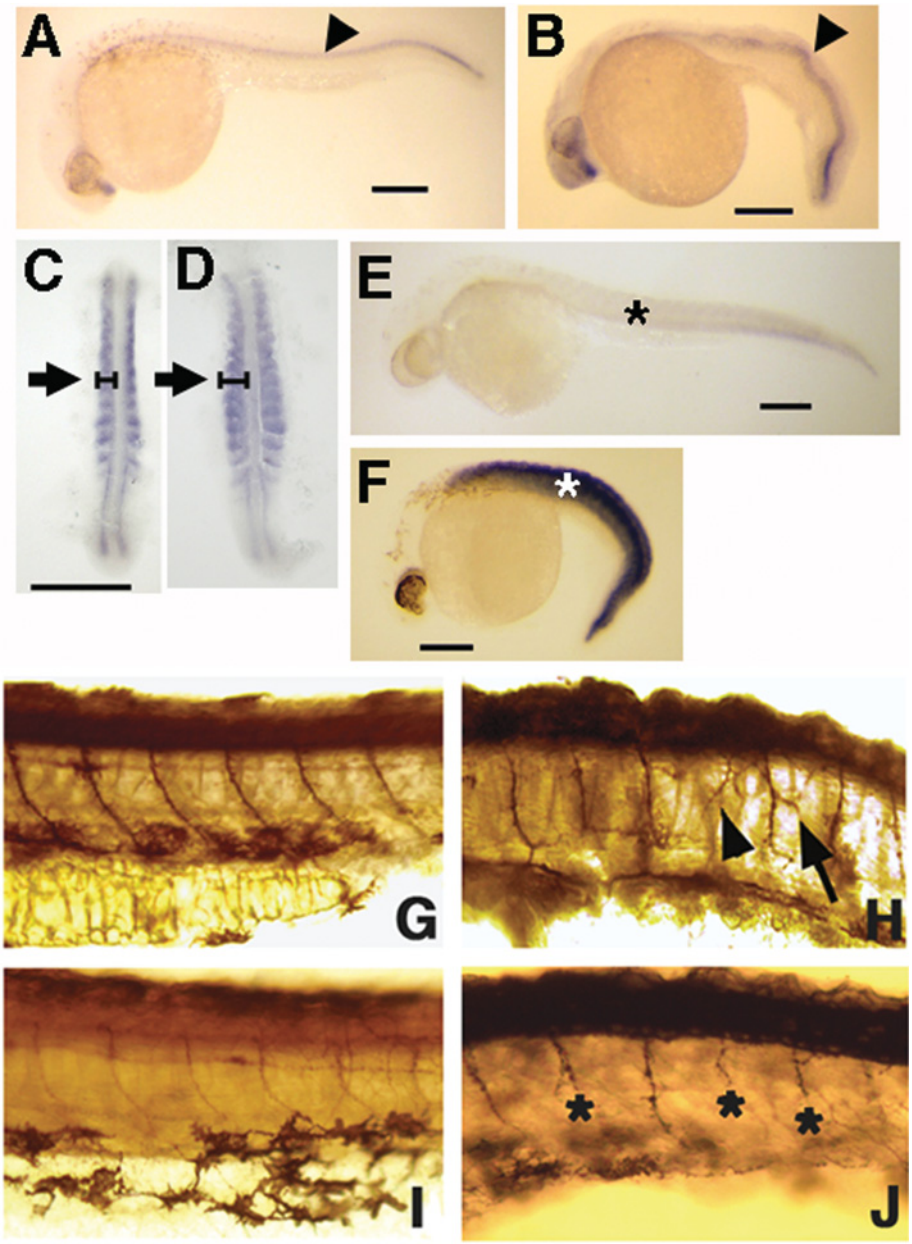

Figure 7 Expression patterns of *shha* and *myod* (A–F) and projection of ventral motor axons (G–J) in wild-type embryos and *C4ST-1* morphants

(**A**–**F**) Expression of *shha* (**A**, **B**) and *myod* (**C**–**F**) in wild-type embryos (**A**, **C**, **E**) and *C4ST-1* morphants (**B**, **D**, **F**) was detected by whole-mount *in situ* hybridization. There was no difference in notochordal *shha* expression (arrowhead) between wild-type embryos (**A**) and *C4ST-1* morphants (**B**) at 24 hpf. At 16 hpf, the expression pattern of *myod* in the morphants (**D**) had an intrinsically wild-type appearance (**C**), except for a slight lateral expansion (arrow). Of particular note, *myod* expression (asterisk) in the somites had largely disappeared in 30 hpf wild-type embryos (**E**), whereas it remained strong in 30 hpf *C4ST-1* morphants (**F**). (**A**, **B**, **E**, **F**) Lateral view, anterior to the left. (**C**, **D**) Dorsal view, anterior to the top. Scale bars, 200 μm. (**G**–**J**) Lateral views (anterior to the left, dorsal to the top) of trunk (**G**, **H**) and tail (**I**, **J**) regions in 48–51 hpf wild-type embryos (**G**, **I**) and the *C4ST-1* morphants (**H**, **J**) immunostained with anti-acetylated α-tubulin. In the *C4ST-1* morphants, truncated (asterisks), misrouted (arrowhead) and side-branched axons (arrow) were observed.

translation system revealed that MO1 inhibited the translation of C4ST-1 but not that of C4ST-2 or D4ST-1 (Figure 4), suggesting that *in vivo* expression of the two isoenzymes of C4ST-1 was not interfered with by the treatment with MO1. It should be noted that the overexpression of either C4ST-2 or D4ST-1, unlike C4ST-1, in sog9 cells cannot restore the proportion of 4-O-sulfated CS and amount of CS [18]. Together, these results suggest that C4ST-1 is the predominant sulfotransferase regulating the 4-O-sulfation and amount of CS during embryogenesis in zebrafish, as in mammals.

A previous immunohistochemical study has documented that CS is abundantly distributed at the interface between the notochord and individual somites [22]. In the present study, we also found the preferential expression of *C4ST-1* in the rostrocaudal axis including notochord and somites (Figure 3), suggesting important roles for CS in developmental processes in the body axis. Indeed, the morphological traits of 48 hpf *C4ST-1* morphants were characterized by a ventrally bent trunk and a twisted tail (Figure 5). Since the expression of the notochordal marker *shha* was unaffected in *C4ST-1* morphants (Figure 7), the notochordal formation appears to proceed normally. On the other hand, an unusually sustained expression of *myod* was observed in the *C4ST-1* morphants even at 30 hpf when the amount of its mRNA was

markedly reduced in the wild-type somites, in concert with formation of skeletal muscle derived from myotomes (Figure 7). Because the myogenic master transcription factor myoD plays essential roles in muscle differentiation [30] and can drive apoptotic pathways as reported by Asakura et al. [37], the perturbed expression of *myod* in the *C4ST-1* morphants may imply an immature developmental state of myotomes and/or disruption of the somitic musculature accompanied by excessive stimulation of the apoptotic cascade, leading to the aberrant morphology in the trunk and tail.

The defects in somites with persistent expression of *myod*, which were evoked by the functional knockdown of *C4ST-1*, have been also reported for zebrafish embryos injected with MOs, which inhibited functions of HS6ST-2, one of the sulfotransferases involved in Hep/HS (heparan sulfate) biosynthesis [38,39]. HS-PGs play roles in various cellular signalling pathways through the high-affinity binding of HS moieties to diverse Hep-binding proteins including growth factors, cytokines and morphogens [40,41]. Recent studies have demonstrated that CS also possesses the capacity to bind various Hep-binding proteins [9,41]. In fact, signalling pathways involving TGFβ (transforming growth factor β) and BMP (bone morphogenetic protein) are dramatically affected in growth plates of *C4ST-1*-deficient mice [19]. Hence, the apparently similar muscular defects in both morphants might be indicative of partially overlapping or compensatory functions of CS and HS in the regulation of local signalling pathways via Hep-binding myogenic morphogens such as hedgehog and Wnt [42,43]. Most recently, Nadanaka et al. [44] reported that the decreased Wnt-3a signalling in sog9 cells lacking *C4ST-1* mRNA is recovered by the introduction of C4ST-1, providing strong support to the notion that the fine structures of CS formed by C4ST-1 are required for efficient signalling inputs mediated by multiple morphogens.

C4ST-1 has been screened as one of the target genes induced by BMP signalling during differentiation of mouse embryonic stem cells [45]. This indicates that C4ST-1 is one of the essential modulators in a sequence of the BMP-dependent cell fate decisions. In zebrafish, BMPs are known to be key regulators of posterior (i.e. trunk and tail) mesoderm patterning, as typified by zebrafish mutants lacking *bmp2b* that do not form a tail [46]. In view of generally mild but definitive phenotypic abnormalities biased to trunk and tail in *C4ST-1* morphants, C4ST-1 might also be one of the downstream targets of the BMP signalling in the posterior half of the body axis and might play important roles in at least several developmental processes induced by BMPs. Therefore elucidation of the transcriptional regulatory mechanism for *C4ST-1* will provide insights into how C4ST-1 participates in body axis formation including muscle development.

Emerging evidence suggests that CS-PGs are crucial environmental modulators in the nervous system of vertebrates. During neuronal development and regeneration, they have apparently contradictory roles as major inhibitors of axonal pathfindings and regeneration and as neuritogenic molecules [2,3]. These functions are exerted mainly through their CS moieties [2,3,9,10]. During zebrafish embryogenesis, CS is abundantly distributed at the interface between the notochord and somites where ventral motor axons located in the middle of each spinal cord hemisegment project into ventral muscle [22]. As reported previously [23], elimination of CS in the trunk by injection with chondroitinase ABC induces axonal projections with abnormal side branches, indicating that CS constrains the outgrowth of the ventral motor nerves through its inhibitory role as a physical barrier or a repulsive cue for axonal growth. In the present study, aberrant axonal outgrowth of ventral motor neurons was also observed in *C4ST-1* morphants (Figure 7). However, the most common abnormality was characterized by truncated axons rather than abnormally branched and misrouted axons (Table 3). One explanation for this discrepancy is that a low but significant level of CS in the trunk of *C4ST-1* morphants supports fasciculation of the ventral motor nerves, preventing the formation of side branches, whereas a nearly complete loss of CS by treatment with chondroitinase ABC does not. Furthermore, in view of the requirement of myotome-derived cues for the migration of motor axons [24,47], we cannot rule out the possibility that defects in muscle development in *C4ST-1* morphants led to additional indirect effects on the axonal pathfindings, because it has been reported that there was no damage in either the notochord or somites in chondroitinase-treated zebrafish embryos [23].

Although the precise molecular basis of the axonal pathfindings of ventral motor nerves involving 4-O-sulfated CS remains unclear, the high incidence of truncated axons, probably representing axons straying from their pathways, in *C4ST-1* morphants suggests potential bifunctional roles of CS not only as a repulsive cue but also as a permissive/attractive guidance cue for specific axons, as described above. In fact, a substrate uniformly precoated with oversulfated CS variants promoted the outgrowth of neurites in rodent embryonic hippocampal neurons, at least in part, by capturing and presenting several Hep-binding growth factors to neurons [2,3,9]. In addition, habenula nucleus axons derived from the developing rat diencephalon were also able to extend over a substrate precoated with a relatively high concentration of CS-PGs [48]. Interestingly, a CS-PG-coated substrate coexisting with sema5A (semaphorin 5A), a bifunctional guidance cue, serves as an inhibitory cue for habenula nucleus axons, resulting from conversion of the attractive property of sema5A into an inhibitory one through its specific interaction with the CS moieties of CS-PGs [48]. Therefore further exploration of CS-interacting molecules in the extracellular matrix and unidentified functional CS receptor(s) is required for a better understanding of the apparent contradictory neuroregulatory functions of CS.

In contrast with *C4ST-1* morphants and chondroitinase-treated embryos, functional knockdown of zygotic *ChSy-1* (chondroitin synthase-1), which encodes one of the glycosyltransferases involved in the biosynthesis of the chondroitin backbone, has been reported to have no significant effects on the pathfinding of the motor axons, although CS immunoreactivity was reduced in the morphants [47]. Recently, Izumikawa et al. [49,50] demonstrated that chondroitin polymerization can be achieved by any two combinations of four ChSy family members including ChSy-1. Therefore, if similar biosynthetic machinery is encoded by the zebrafish genome, a single knockdown of ChSy family members may not always lead to a drastic reduction in the amount of CS, which provokes developmental defects. Consequently, our results in conjunction with earlier studies [18,19,23] strongly suggest the critical functions of C4ST-1 in CS biosynthesis and in zebrafish embryogenesis. Thus further analysis focusing on C4ST-1 will facilitate our understanding of the molecular mechanisms underlying the development and pathology of various diseases involving CS.

ACKNOWLEDGEMENTS

We thank Junko Fukuda, Saki Sato and Shunsuke Kataoka for technical assistance.

FUNDING

This work was supported in part by a Scientific Promotion Fund from the Japan Private School Promotion Foundation, Grants-in-Aid for Encouragement of Young Scientists

[numbers 20790080 and 18790073; to T. M.] from the MEXT (Ministry of Education, Culture, Sports, Science and Technology) of Japan, a grant from the Uehara Memorial Foundation (to T. M.), and a Grant-in-aid for Scientific Research-B [number 20390019; to K. S.] and the CREST (Core Research for Evolutional Science and Technology) programme of the JST (Japan Science and Technology Agency; to K. S.).

REFERENCES

1 Iozzo, R. V. (1998) Matrix proteoglycans: from molecular design to cellular function. Annu. Rev. Biochem. **67**, 609–652
2 Sugahara, K., Mikami, T., Uyama, T., Mizuguchi, S., Nomura, K. and Kitagawa, H. (2003) Recent advances in the structural biology of chondroitin sulfate and dermatan sulfate. Curr. Opin. Struct. Biol. **13**, 612–620
3 Sugahara, K. and Mikami, T. (2007) Chondroitin/dermatan sulfate in the central nervous system. Curr. Opin. Struct. Biol. **17**, 536–545
4 Schwartz, N. B. and Domowicz, M. (2002) Chondrodysplasias due to proteoglycan defects. Glycobiology **12**, 57R–68R
5 Uyama, T., Kitagawa, H. and Sugahara, K. (2007) Biosynthesis of glycosaminoglycans and proteoglycans. In Comprehensive Glycoscience, Volume 3 (Kamerling, J. P., ed.), pp. 79–104, Elsevier, Amsterdam
6 Mark, M. P., Baker, J. R., Kimata, K. and Ruch, J. V. (1990) Regulated changes in chondroitin sulfation during embryogenesis: an immunohistochemical approach. Int. J. Dev. Biol. **34**, 191–204
7 Kitagawa, H., Tsutsumi, K., Tone, Y. and Sugahara, K. (1997) Developmental regulation of the sulfation profile of chondroitin sulfate chains in the chicken embryo development. J. Biol. Chem. **272**, 31377–31381
8 Mitsunaga, C., Mikami, T., Mizumoto, S., Fukuda, J. and Sugahara, K. (2006) Chondroitin sulfate/dermatan sulfate hybrid chains in the development of cerebellum. Spatiotemporal regulation of the expression of critical disulfated disaccharides by specific sulfotransferases. J. Biol. Chem. **281**, 18942–18952
9 Mikami, T. and Sugahara, K. (2006) The biological importance of specific sulfation of chondroitin sulfate/dermatan sulfate in their functional expression. Trends Glycosci. Glycotechnol. **18**, 165–183
10 Gama, C. I., Tully, S. E., Sotogaku, N., Clark, P. M., Rawat, M., Vaidehi, N., Goddard, III, W. A., Nishi, A. and Hsieh-Wilson, L. C. (2006) Sulfation patterns of glycosaminoglycans encode molecular recognition and activity. Nat. Chem. Biol. **2**, 467–473
11 Kusche-Gullberg, M. and Kjellén, L. (2003) Sulfotransferase in glycosaminoglycan biosynthesis. Curr. Opin. Struct. Biol. **13**, 605–611
12 Maccarana, M., Olander, B., Malmström, J., Tiedemann, K., Aebersold, R., Lindahl, U., Li, J. P. and Malmström, A. (2006) Biosynthesis of dermatan sulfate: chondroitin-glucuronate C5-epimerase is identical to SART2. J. Biol. Chem. **281**, 11560–11568
13 Yamauchi, S., Mita, S., Matsubara, T., Fukuta, M., Habuchi, H., Kimata, K. and Habuchi, O. (2000) Molecular cloning and expression of chondroitin 4-sulfotransferase. J. Biol. Chem. **275**, 8975–8981
14 Hiraoka, N., Nakagawa, H., Ong, E., Akama, T. O., Fukuda, M. N. and Fukuda, M. (2000) Molecular cloning and expression of two distinct human chondroitin 4-*O*-sulfotransferases that belong to the HNK-1 sulfotransferase gene family. J. Biol. Chem. **275**, 20188–20196
15 Kang, H.-G., Evers, M. R., Xia, G., Baenziger, J. U. and Schachner, M. (2002) Molecular cloning and characterization of chondroitin-4-*O*-sulfotransferase-3. J. Biol. Chem. **277**, 34766–34772
16 Evers, M. R., Xia, G., Kang, H. G., Schachner, M. and Baenziger, J. U. (2001) Molecular cloning and characterization of a dermatan-specific *N*-acetylgalactosamine 4-*O*-sulfotransferase. J. Biol. Chem. **276**, 36344–36353
17 Mikami, T., Mizumoto, S., Kago, N., Kitagawa, H. and Sugahara, K. (2003) Specificities of three distinct human chondroitin/dermatan *N*-acetylgalactosamine 4-*O*-sulfotransferases demonstrated using partially desulfated dermatan sulfate as an acceptor. J. Biol. Chem. **278**, 36115–36127
18 Uyama, T., Ishida, M., Izumikawa, T., Trybala, E., Tufaro, F., Bergström, T., Sugahara, K. and Kitagawa, H. (2006) Chondroitin 4-*O*-sulfotransferase-1 regulates E disaccharide expression of chondroitin sulfate required for herpes simplex virus infectivity. J. Biol. Chem. **281**, 38668–38674
19 Klüppel, M., Wight, T. N., Chan, C., Hinek, A. and Wrana, J. L. (2005) Maintenance of chondroitin sulfation balance by chondroitin-4-sulfotransferase 1 is required for chondrocyte development and growth factor signaling during cartilage morphogenesis. Development **132**, 3989–4003
20 Nüsslein-Volhard, C., Gilmour, D. T. and Dahm, R. (2002) Introduction: zebrafish as a system to study development and organogenesis. In Zebrafish (Nüsslein-Volhard, C. and Dahm R., eds), pp. 1–5, Oxford University Press, New York
21 Grunwald, D. J. and Eisen, J. S. (2002) Headwaters of the zebrafish – emergence of a new model vertebrate. Nat. Rev. Genet. **3**, 717–724
22 Bernhardt, R. R., Goerlinger, S., Roos, M. and Schachner, M. (1998) Anterior–posterior subdivision of the somite in embryonic zebrafish: implications for motor axon guidance. Dev. Dyn. **213**, 334–347
23 Bernhardt, R. R. and Schachner, M. (2000) Chondroitin sulfates affect the formation of the segmental motor nerves in zebrafish embryos. Dev. Biol. **221**, 206–219
24 Schneider, V. A. and Granato, M. (2003) Motor axon migration: a long way to go. Dev. Biol. **263**, 1–11
25 Stickney, H. L., Barresi, M. J. and Devoto, S. H. (2000) Somite development in zebrafish. Dev. Dyn. **219**, 287–303
26 Inohaya, K., Takano, Y. and Kudo, A. (2007) The teleost intervertebral region acts as a growth center of the centrum: *in vivo* visualization of osteoblasts and their progenitors in transgenic fish. Dev. Dyn. **236**, 3031–3046
27 Kimmel, C. B., Ballard, W. W., Kimmel, S. R., Ullmann, B. and Schilling, T. F. (1995) Stages of embryonic development of the zebrafish. Dev. Dyn. **203**, 253–310
28 Kitagawa, H., Egusa, N., Tamura, J., Kusche-Gullberg, M., Lindahl, U. and Sugahara, K. (2001) *rib-2*, a *Caenorhabditis elegans* homolog of the human tumor suppressor EXT genes encodes a novel alpha1,4-*N*-acetylglucosaminyltransferase involved in the biosynthetic initiation and elongation of heparan sulfate. J. Biol. Chem. **276**, 4834–4838
29 Roelink, H., Augsburger, A., Heemskerk, J., Korzh, V., Norlin, S., Ruiz i Altaba, A., Tanabe, Y., Placzek, M., Edlund, T., Jessell, T. M. and Dodd, J. (1994) Floor plate and motor neuron induction by *vhh-1*, a vertebrate homolog of *hedgehog* expressed by the notochord. Cell **76**, 761–775
30 Weinberg, E. S., Allende, M. L., Kelly, C. S., Abdelhamid, A., Murakami, T., Andermann, P., Doerre, O. G., Grunwald, D. J. and Riggleman, B. (1996) Developmental regulation of zebrafish *MyoD* in wild-type, *no tail* and *spadetail* embryos. Development **122**, 271–280
31 Schlte-Merker, S. (2002) Looking at embryos. In Zebrafish (Nüsslein-Volhard, C. and Dahm, R., eds), pp. 39–58, Oxford University Press, New York
32 Nasevicius, A. and Ekker, S. C. (2000) Effective targeted gene 'knockdown' in zebrafish. Nat. Genet. **26**, 216–220
33 Yamada, S., Okada, Y., Ueno, M., Iwata, S., Deepa, S. S., Nishimura, S., Fujita, M., Van Die, I., Hirabayashi, Y. and Sugahara, K. (2002) Determination of the glycosaminoglycan-protein linkage region oligosaccharide structures of proteoglycans from *Drosophila melanogaster* and *Caenorhabditis elegans*. J. Biol. Chem. **277**, 31877–31886
34 Kinoshita, A. and Sugahara, K. (1999) Microanalysis of glycosaminoglycan-derived oligosaccharides labeled with a fluorophore 2-aminobenzamide by high-performance liquid chromatography: application to disaccharide composition analysis and exosequencing of oligosaccharides. Anal. Biochem. **269**, 367–378
35 Souza, A. R., Kozlowski, E. O., Cerqueira, V. R., Castelo-Branco, M. T., Costa, M. L. and Pavão, M. S. (2007) Chondroitin sulfate and keratan sulfate are the major glycosaminoglycans present in the adult zebrafish *Danio rerio* (Chordata-Cyprinidae). Glycoconj. J. **24**, 521–530
36 Stemple, D. L., Solnica-Krezel, L., Zwartkruis, F., Neuhauss, S. C. F., Schier, A. F., Malicki, J., Stainier, D. Y. R., Abdelilah, S., Rangini, Z., Mountcastle-Shah, E. and Driever, W. (1996) Mutations affecting development of the notochord in zebrafish. Development **123**, 117–128
37 Asakura, A., Hirai, H., Kablar, B., Morita, S., Ishibashi, J., Piras, B. A., Christ, A. J., Verma, M., Vineretsky, K. A. and Rudnicki, M. A. (2007) Increased survival of muscle stem cells lacking the *MyoD* gene after transplantation into regenerating skeletal muscle. Proc. Natl. Acad. Sci. U.S.A. **104**, 16552–16557
38 Bink, R. J., Habuchi, H., Lele, Z., Dolk, E., Joore, J., Rauch, G. J., Geisler, R., Wilson, S. W., den Hertog, J., Kimata, K. and Zivkovic, D. (2003) Heparan sulfate 6-*O*-sulfotransferase is essential for muscle development in zebrafish. J. Biol. Chem. **278**, 31118–31127
39 Chen, E., Stringer, S. E., Rusch, M. A., Selleck, S. B. and Ekker, S. C. (2005) A unique role for 6-*O* sulfation modification in zebrafish vascular development. Dev. Biol. **284**, 364–376
40 Esko, J. D. and Selleck, S. B. (2002) Order out of chaos: assembly of ligand binding sites in heparan sulfate. Annu. Rev. Biochem. **71**, 435–471
41 Raman, R., Sasisekharan, V. and Sasisekharan, R. (2005) Structural insights into biological roles of protein–glycosaminoglycan interactions. Chem. Biol. **12**, 267–277
42 Feng, X., Adiarte, E. G. and Devoto, S. H. (2006) Hedgehog acts directly on the zebrafish dermomyotome to promote myogenic differentiation. Dev. Biol. **300**, 736–746
43 Pownall, M. E., Gustafsson, M. K. and Emerson, Jr, C. P. (2002) Myogenic regulatory factors and the specification of muscle progenitors in vertebrate embryos. Annu. Rev. Cell Dev. Biol. **18**, 747–783

44 Nadanaka, S., Ishida, M., Ikegami, M. and Kitagawa, H. (2008) Chondroitin 4-*O*-sulfotransferase-1 modulates Wnt-3a signaling through control of E disaccharide expression of chondroitin sulfate. J. Biol. Chem. **283**, 27333–27343
45 Klüppel, M., Vallis, K. A. and Wrana, J. L. (2002) A high-throughput induction gene trap approach defines C4ST as a target of BMP signaling. Mech. Dev. **118**, 77–89
46 Mullins, M. C., Hammerschmidt, M., Kane, D. A., Odenthal, J., Brand, M., van Eeden, F. J., Furutani-Seiki, M., Granato, M., Haffter, P., Heisenberg, C. P. et al. (1996) Genes establishing dorsoventral pattern formation in the zebrafish embryo: the ventral specifying genes. Development **123**, 81–93
47 Zhang, I., Lefebvre, J. L., Zhao, S. and Granato, M. (2004) Zebrafish *unplugged* reveals a role for muscle-specific kinase homologs in axonal pathway choice. Nat. Neurosci. **7**, 1303–1309
48 Kantor, D. B., Chivatakarn, O., Peer, K. L., Oster, S. F., Inatani, M., Hansen, M. J., Flanagan, J. G., Yamaguchi, Y., Sretavan, D. W., Giger, R. J. and Kolodkin, A. L. (2004) Semaphorin 5A is a bifunctional axon guidance cue regulated by heparan and chondroitin sulfate proteoglycans. Neuron **44**, 961–975
49 Izumikawa, T., Uyama, T., Okuura, Y., Sugahara, K. and Kitagawa, H. (2007) Involvement of chondroitin sulfate synthase-3 (chondroitin synthase-2) in chondroitin polymerization through its interaction with chondroitin synthase-1 or chondroitin-polymerizing factor. Biochem. J. **403**, 545–552
50 Izumikawa, T., Koike, T., Shiozawa, S., Sugahara, K., Tamura, J. and Kitagawa, H. (2008) Identification of chondroitin sulfate glucuronyltransferase as chondroitin synthase-3 involved in chondroitin polymerization: chondroitin polymerization is achieved by multiple enzyme complexes consisting of chondroitin synthase family members. J. Biol. Chem. **283**, 11396–11406

Received 11 August 2008/12 December 2008; accepted 6 January 2009
Published as BJ Immediate Publication 6 January 2009, doi:10.1042/BJ20081639